

New Tests of Magnetospheric Accretion in T Tauri Stars

Christopher M. Johns–Krull¹ and April D. Gafford²

*Space Sciences Laboratory, University of California, Berkeley, CA
94720, cmj@ssl.berkeley.edu, agafford@ssl.berkeley.edu*

ABSTRACT

We examine 3 analytic theories of magnetospheric accretion onto classical T Tauri stars under the assumption that the magnetic field strength does not vary appreciably from star to star. From these investigations we derive predicted relationships among the stellar mass, radius, rotation period, and disk accretion rate. Data from 5 studies of the accretion parameters of CTTSs are used to test the predicted correlations. We generally find that the data do not display the predicted correlations except for that predicted by the model of Shu et al. as detailed by Ostriker and Shu and extended here to include non-dipole field topologies. Their identification of the trapped flux as an important quantity in the model appears to be critical for reconciling the observed data to the theory. While the data do generally support the extended Ostriker and Shu predictions, only one of the two studies for which the requisite data exist show the highest correlation when considering all the relevant parameters. This suggests great care must be taken when trying to use existing observations to test the theory.

Subject headings: accretion, accretion disks — stars: pre–main–sequence —

1. Introduction

Classical T Tauri stars (CTTSs) appear to be roughly solar mass pre-main sequence stars still surrounded by disks of material which actively accrete onto the central star. It is within such disks that solar systems form. Understanding the processes through which young stars interact with and eventually disperse their disks is critical for understanding the rotational evolution of stars and the formation of planets. A key question is to understand how young stars can accrete large amounts of disk material with high specific angular momentum, yet maintain rotation rates that are observed to be relatively slow (e.g. Hartmann & Stauffer 1989, Edwards et al. 1994). Current models state that this process proceeds via magnetospheric accretion: stellar magnetic fields truncate the inner disk and channel accreting material onto the stellar surface, preferentially at high latitude. More generally in astrophysics, magnetized accretion onto a central source is a common theme in various contexts including accretion onto white dwarfs (e.g. AM Her stars – Wickramasinghe & Ferrario 2000), pulsars (pulsating X-ray sources – Ghosh & Lamb 1979), and possibly black holes at the center of active galactic nuclei (e.g. Koide, Shibata, & Kudoh 1999). Detailed tests of magnetospheric accretion theory are necessary for understanding CTTSs as well as these other classes of objects.

¹Now at Department of Physics and Astronomy, Rice University, 6100 Main St., MS-61, Houston, TX 77005

²Also Department of Physics and Astronomy, San Francisco State University, San Francisco, CA 94132

Support for magnetospheric accretion in CTTSs is significant. Current models can account for the relatively slow rotation of most CTTSs (Camenzind 1990; Königl 1991; Shu et al. 1994; Paatz & Camenzind 1996). Studies of the spectroscopic and photometric variability of CTTSs often suggest magnetically controlled accretion (e.g. Bertout, Basri, & Bouvier 1988; Bertout et al. 1996; Herbst, Bailer–Jones, & Mundt 2001; Alencar, Johns–Krull, & Basri 2001) with the magnetic axis inclined to the rotation axis in some cases (e.g. Kenyon et al. 1994, Johns–Krull & Basri 1995, Bouvier et al. 1999). Models of high resolution Balmer line profiles, computed in the context of magnetospheric accretion, reproduce many aspects of observed line profiles (Muzerolle, Calvet, & Hartmann 1998, Muzerolle et al. 2000). T Tauri stars are observed to be strong X-ray sources indicating the presence of strong magnetic fields on their surfaces (see Feigelson & Montmerle 1999 for a review), and CTTSs are observed to have strong surface magnetic fields (Guenther et al. 1999; Johns–Krull et al. 1999b; Johns–Krull et al. 2001), and strong magnetic fields have been observed in the formation region of the He I emission line at 5876 Å (Johns–Krull et al. 1999a; Johns–Krull & Valenti 2000), which is believed to be produced in a shock near the stellar surface as the disk material impacts the star.

Despite these successes, open issues remain. Current theoretical models assume a dipole geometry for the stellar magnetic field; however, Johns–Krull et al. (1999a) and Johns–Krull and Valenti (2001) show that the surface fields on BP Tau and TW Hya are not dipolar. On the other hand, it is expected that the dipole component of the field should dominate at distance from the star where the interaction with the disk is taking place, so this may not contradict current theory. Even in the case of the complex magnetic topology of the Sun, the dipole component appears to become dominant at $2.5R_{\odot}$ or closer (e.g. Luhmann et al. 1998). For expected disk truncation radii of $3 - 6 R_*$ in CTTSs, this suggests the dipole component will govern the stellar interaction with the disk. On the other hand, Stassun et al. (1999) find no correlation between rotation period and IR signatures of circumstellar disks in a sample of 254 stars in Orion, leading them to question the validity of magnetically mediated disk locking which is intrinsic to magnetospheric accretion theory. Bertout and Mennessier (1996) review points in favor of both the magnetospheric accretion model and the original axisymmetric, equatorial boundary layer model (based on the work of Lynden–Bell & Pringle 1974) which came before. While the magnetospheric model remains the favorite in the current literature, Bertout and Mennessier (1996) conclude that the existing data does not favor either model. Thus, the overall success of magnetospheric accretion as the best description of accretion onto CTTSs remains in some doubt.

The current equilibrium theories of magnetospheric accretion predict specific relationships between the stellar mass (M_*), radius (R_*), rotation period (P_{rot}), magnetic field (B_*), and mass accretion rate (\dot{M}) (e.g. Johns–Krull et al. 1999b). Unfortunately, observation of all these quantities are only available for a handful of stars, with magnetic field measurements the most lacking. One could look for correlations among the other quantities to test the theories. Ghosh (1995) investigated the rotation and accretion properties of a number of T Tauri stars (TTSs) by assuming a dynamo relation for TTS magnetic fields in terms of Rossby number (convective turnover time divided by rotation period) since there were almost no magnetic field measurements for TTSs available at the time. Ghosh (1995) found that TTSs generally cluster below the limiting rotation rate as is to be expected; however, no clear correlations were seen in the data. Johns–Krull, Valenti, and Linsky (2001) have shown that TTS Rossby numbers generally place them in the region of saturated magnetic activity compared to main sequence and evolved stars, so it is not clear that parameterizing the stellar field in terms of the Rossby number is appropriate for these stars. Furthermore, TTSs do not show a large range of magnetic field properties as described below. While we are unaware of any other systematic studies along this line, Muzerolle, Calvet, and Hartmann (2001) note that current theory predicts a correlation between rotation period and mass accretion rate which has not been observed. Muzerolle et al. (2001) suggest that

variations in the stellar magnetic field strength from star to star may account for the lack of correlation.

Johns–Krull et al. (2001) show that the mean photospheric magnetic fields of 6 TTs range only between 2.1 and 2.7 kG, suggesting a surprising uniformity to the field strengths on these stars. The field on T Tau obtained by Guenther et al. (1999) also falls in this range. These observations are of the magnetic field averaged over the entire stellar surface, while for the current discussion we are most interested in the field in the actual accretion zones. Johns–Krull et al. (1999a) discovered a magnetic field in the He I 5876Å emission line on BP Tau from observations of circular polarization, arguing that the narrow component of this line likely forms in the postshock region as material accretes onto the stellar surface (see also Hartmann, Hewett, & Calvet 1994 and Lamzin 1995). The field detected is 2.5 kG, which is a lower limit to the true field due to the unknown angle between the field lines and the line of sight. Johns–Krull et al. (2001) also present similar spectropolarimetric observations of 4 CTTSs over 6 nights, finding fields in the He I line formation region that vary smoothly with time, probably due to stellar rotation which suggests the fields participating in the accretion flow are stable at least on a rotational time scale (see also Valenti, Johns–Krull, & Hatzes 2001). In all cases, the field determined from the He I polarization is equal to or lower than the mean photospheric field, as is expected if the fields are in fact the same but the He I measurement is reduced as a result of field line inclination to the line of sight.

As mentioned above, the theoretical relationships predicted by magnetospheric accretion theory involve many parameters, not just rotation period and mass accretion rate. Since all the existing observational data suggests relative uniformity of surface magnetic field strengths on CTTSs (at least in Taurus where the most detailed studies have taken place), we have examined several sources of data from the literature to look for the expected correlations assuming the field strength is in fact constant from star to star. This constancy of the magnetic field may represent some limit to the dynamo operating in these young stars. Certainly, the details of such a dynamo are far from well understood; however, Johns–Krull et al. (2001) show that within the context of other active stars, TTs are expected to show saturated magnetic activity based on their rotation and convective parameters, perhaps giving further justification to assuming a constant magnetic field. In §2 we review the predicted relationships between the various stellar and accretion parameters. In §3 we examine literature compilations of the requisite parameters for testing the predicted correlations. Section 4 presents the analysis of this data. In §5 we discuss our results, and our conclusions are given in §6.

2. Magnetospheric Accretion Predictions

Johns–Krull et al. (1999b) examined three analytic theories (Königl 1991, Cameron & Campbell 1993, Shu et al. 1994) of magnetospheric accretion, presenting equations for the stellar magnetic field strength as a function of M_* , R_* , P_{rot} , and \dot{M} . These studies are outgrowths of the pioneering work done by Ghosh and Lamb (1979) on accreting neutron stars. The work of Königl (1991) and Cameron and Campbell (1993) are very closely related to that of Ghosh and Lamb (1979) in that these papers only consider accretion onto the star. The Shu et al. (1994) work is different in that it is an integrated theory of accretion onto the central star plus a wind which is driven off the disk at the truncation point (the X-region). While coefficients representing such things as the efficiency of magnetic coupling to the disk vary from one study to the other, the predictions from Königl (1991) and Shu et al. (1994) depended in the same way on the above stellar and accretion parameters for an assumed dipolar magnetic field. Holding the stellar magnetic field constant, Königl (1991) and Shu et al. (1994) predict that

$$R_*^3 \propto M_*^{5/6} \dot{M}^{1/2} P_{rot}^{7/6}. \quad (1)$$

In the case of Cameron and Campbell (1993), the relationship is

$$R_*^3 \propto M_*^{2/3} \dot{M}^{23/40} P_{rot}^{29/24}, \quad (2)$$

which is very similar in its dependencies to Königl (1991) and Shu et al. (1994). In fact, scatter plots created using equation (2) are virtually identical to those created using equation (1). Therefore, we only show plots based on equation (1); however, the results for equation (2) are cited in the tables and discussed in the text.

In a more detailed analysis of the magnetospheric accretion flow itself, Ostriker and Shu (1995) identified the importance of the notion of trapped flux in the Shu et al. (1994) theory. While still assuming a dipole stellar field, Ostriker and Shu noted that what their theory really predicted was the amount of magnetic flux trapped in the X-region. In their preferred model, this is 1.5 times the magnetic flux which would thread the disk exterior to the truncation point (the co-rotation radius in their model) in an undisturbed dipole field. For the system to remain in equilibrium, this is the flux that must be trapped in the X-region independent of the topology of the magnetic field on the stellar surface. Armed with this information, we can derive a new relationship among the observable parameters which is unique to the Ostriker and Shu (1995) treatment of the Shu et al. (1994) theory.

Re-writing equation (4.1) of Ostriker and Shu (1995) for the radius of the X-point, R_x , we have

$$R_x = \Phi_{dx}^{-4/7} \left(\frac{\mu_*^4}{GM_* \dot{M}_D^2} \right)^{1/7} \quad (3)$$

where $\Phi_{dx}^{-4/7}$ is a constant evaluated by Ostriker and Shu (1995) to be 0.923 in their preferred model, μ_* is the dipole moment of the star, G the gravitational constant, and \dot{M}_D is the mass accretion rate through the disk. The general form of this equation is well known from many studies of accretion onto compact objects (see for example White & Stella 1988). In the Shu et al. (1994) theory, the disk mass accretion rate is not equal to the accretion rate onto the star (the quantity measured in the observations described below) since the theory also incorporates a magnetocentrifugally driven wind from the X-region; however, the two are related by a factor of order 2/3.

For a purely dipolar field, the magnetic flux threading the disk exterior to the point R_x is

$$\phi_x = \frac{2\pi\mu_*}{R_x}. \quad (4)$$

In the preferred model of Ostriker and Shu (1995) the total flux trapped in the X-region is $\phi_t = 1.5\phi_x$, of which a third participates in the accretion funnel flow of material onto the star (another third is in the dead zone, and the final third is part of the wind). Thus, the magnetic flux threading the X-region which directs disk material onto the star is $0.5\phi_x$ independent of the exact topology of the field at the stellar surface, as long as the dipole dominates in the X-region. Equating this magnetic flux to that on the star in the accretion zones, we have

$$B_* A_* = 0.5\phi_x = \frac{\pi\mu_*}{R_x} \quad (5)$$

where A_* is the area on the surface of the star on which the accreting disk material falls.

If we recall that R_x in the Shu et al. (1994) theory is the co-rotation radius, where the Keplerian angular velocity in the disk is equal to the angular velocity of stellar rotation, we can solve equation (5) for μ_* , substitute the result into equation (3) and get

$$\begin{aligned} B_* A_* &= 2^{-1/2} \pi^{1/2} G^{1/2} \Phi_{dx}^{1/2} M_*^{1/2} \dot{M}_D^{1/2} P_{rot}^{1/2} \\ &= 8.88 \times 10^{24} \left(\frac{M_*}{M_\odot} \right)^{1/2} \left(\frac{\dot{M}_D}{10^{-7} M_\odot \text{ yr}^{-1}} \right)^{1/2} \left(\frac{P_{rot}}{1 \text{ day}} \right)^{1/2} \text{ G cm}^2 \end{aligned} \quad (6)$$

after some manipulation. In this paper, we assume B_* does not vary from star to star and $A_* = 4\pi R_*^2 f_{acc}$ where f_{acc} is the filling factor of accretion zones, so equation (6) implies

$$R_*^2 f_{acc} \propto M_*^{1/2} \dot{M}^{1/2} P_{rot}^{1/2} \quad (7)$$

as a unique prediction of the Shu et al. (1994) theory as detailed by Ostriker and Shu (1995) and expanded here to incorporate a non-dipole field topology near the stellar surface. In equation (7), \dot{M} is the mass accretion rate onto the star and $\dot{M} = \alpha \dot{M}_D$ where $\alpha \sim 2/3$ since the wind carries away about one third of the *disk* accretion rate (Shu et al. 1994). Hartigan, Edwards, and Ghandour (1995) attempted to observationally determine the ratio of mass loss to mass accretion rate, finding a value of 0.01; however, more recent estimates of this ratio are ~ 0.1 (see review of Königl & Pudritz 2000) so the Shu et al. (1994) value seems quite reasonable given the current state of the observations.

In equation (7) above, the filling factor, f_{acc} , is the filling factor of the accretion spots on the stellar surface, which is not the same as the filling factor of the magnetic field. In the theories which use a strict dipole field geometry in which the magnetic axis is aligned with the rotation axis (the typical assumption), the magnetic filling factor is 1.0, but accretion onto the star occurs only in axisymmetric rings located at high latitude. Thus the filling factor of accretion zones is expected to be significantly less than 1.0, and its value is strongly influenced by the small scale topology of the magnetic field at the stellar surface. On the other hand, it is the bright accretion shock emission produced in these regions which is believed to give rise to the UV continuum excess and optical veiling emission seen in CTTSs (e.g. Calvet & Gullbring 1998). As a result, it is possible to observationally determine f_{acc} , and this has been done for reasonably large samples of stars by Valenti, Basri, and Johns (1993) and Calvet and Gullbring (1998). As discussed further below, accurate estimates of f_{acc} are required to test the correlations predicted by equation (7), and these estimates can be difficult to make.

In this paper we focus on the above mentioned theories since they are largely analytic and permit the derivation of relatively simple expressions which show the dependence of stellar and accretion parameters on one another in the equilibrium situation. These expressions can be tested in a rather straightforward way using existing observational data. This is not to suggest that the above studies are the only such studies of magnetospheric accretion in CTTSs. There are a number of others, some of which derive their results from numerical studies of the governing equations (e.g. Paatz & Camenzind 1996), while some focus on the instabilities that can result between the star, its magnetosphere, and the disk which may launch winds and jets (e.g. Hayashi, Shibata, & Matsumoto 1996; Goodson, Winglee, & Böhm 1997; Miller & Stone 1997; Goodson, Böhm, & Winglee 1999; Ferreira, Pelletier, & Appl 2000). These studies are not directly testable in the fashion explored in this paper; however, important tests of many of these works may be possible with variability studies (see Goodson et al. 1999). Finally, we note that CTTSs are variable as has been mentioned in §1. This variability is not accounted for in the equilibrium theories examined in this paper, but is not necessarily evidence that these theories should be abandoned. The theories may be perfectly adequate to describe the average conditions of CTTSs. In this case, we expect to see the predicted correlations in the data, and the variability (as well as measurement error) should produce scatter about the mean relations. It is these correlations we are looking for here.

3. Data Used

The goal of this paper is test the proportionalities predicted in equations (1), (2), and (7) by using data from the literature to look for the predicted correlations. For consistency within each of the studies we

employ, we use the stellar and accretion parameters from each individual study when testing for the predicted correlations instead of trying to come up with a single best estimate for each of the relevant parameters. The rotation periods are all taken from photometric monitoring studies which do not depend on these stellar parameters, so we apply the detected periods to all the accretion data sets.

Mass accretion rates onto large samples of CTTSs have been estimated by Valenti et al. (1993 – hereafter VBJ); Hartigan, Edwards, and Ghandour (1995 – hereafter HEG); Gullbring et al. (1998 – hereafter GHBC); Calvet and Gullbring (1998 – hereafter CG98); and White and Ghez (2001 – hereafter WG01). Of these papers, only VBJ and CG98 estimate the filling factor, f_{acc} , of accreting material on the stellar surface, which is required to test the relationship given in equation (7). CG98 do not separately estimate, T_{eff} , M_* , and R_* , instead using the values tabulated by GHBC which are reproduced in the tables here. For the 4 continuum stars (CW Tau, DG Tau, DL Tau, and DR Tau) from CG98 which are used in this study, CG98 assume $R_* = 2R_\odot$ and $M_* = 0.5M_\odot$, which we use here. In addition, CG98 do not tabulate \dot{M} specifically, but the mass loss rate can be calculated from their equation (11) and the quantities tabulated in the paper. We note that in CG98, they do not perform a detailed fit to the data presented in GHBC, instead adopting the values from their grid of models which gives the best fit to the data as estimated by eye. However, this should be adequate for our purpose of looking for general correlations among different parameters. Rotation period data comes from the following papers in order of preference: Bouvier et al. 1995, Bouvier 1990, Bertout et al. 1996, and Bouvier et al. 1993. Tables 1 through 5 give the final compilation of stars and their relevant parameters for the 5 studies examined here. In a few cases (noted in the tables), required quantities such as the stellar radius are not tabulated in the original studies, but can be estimated from the tabulated stellar luminosity and effective temperature. For those studies which only tabulate spectral type, the spectral type – effective temperature calibration of Johnson (1966) is used in this paper to estimate T_{eff} .

Some of the stars used in this study are now known to be binary, while this was not known to be the case in earlier studies. In addition, pre-main sequence evolutionary tracks have been refined over time, which influences the derivation of stellar parameters. For many of the binaries, their separation is large enough (DK Tau, GK Tau, RW Aur) that they do not fall in the slit used by HEG, while WG01 explicitly take into account the binary nature of these stars. For the studies based on low to medium resolution spectroscopy (VBJ, GHBC, CG98), the slits used were wide enough to encompass both members of the binary systems. However, it is generally the case (DF Tau, DK Tau, GG Tau A, RW Aur) that the primary star dominates the optical and short wavelength light (Mathieu 1994; Ghez, White, & Simon 1997; Duchene et al. 1999; WG01) from which the accretion parameters are derived. As a result, the accretion rates and filling factors apply to the primary in the case of those stars with originally unknown companions. Inclusion of the WG01 results in this study will also serve to see if accurate accounting for binarity significantly changes the results. The use of different pre-main sequence tracks and differences in the extinction corrections used (as well as unknown binaries) between the different studies results in small (generally less than a factor of 2) changes in the stellar mass and radius from one study to the other, but these differences are small compared to the full range of parameters explored in the samples. We choose to use the samples as is since changes made in one parameter can also affect others (such as the mass accretion rate), so here we hope to maintain consistent sets of parameters from one study to the next as we look for general correlations among the parameters.

In addition to observational issues related to the influence of binaries, it is fair to consider the theoretical influence of binary interactions. This paper is concerned with the star-disk interaction, and the theories examined here have the disk accretion rate as a free parameter. Therefore, if CTTSs in binaries have different disk accretion rates compared to single CTTSs, this difference should naturally be accounted for. Theoretical effects studied in CTTS binary systems include disk truncation and circumbinary replenishment

(e.g. Artymowicz & Lubow 1994, 1996) and changes to disk accretion rates (e.g. Ostriker, Shu, & Adams 1992), but most authors consider the star-disk interaction to be the same as for single CTTSs (e.g. Armitage, Clarke, & Tout 1999). Observationally, WG01 find no difference in the accretion rate as a function of binary separation in the range 10 - 1000 AU, and Simon & Prato (1995) find no difference in disk lifetime between binary and single CTTSs. Thus, it is unlikely there is any real difference in the star-disk interaction for CTTSs in relatively wide binaries such as those considered here compared to single CTTSs. As a result, we include both single CTTSs and CTTSs in binaries in the current analysis, but we separate them by plot symbol for clarity. Stars identified as binary in WG01, Mathieu (1994), or Ghez, Neugebauer, and Matthews (1993) are labelled as binary; while stars indicated as single in WG01 are labelled so here.

As mentioned above, VBJ and CG98 are the only studies which determine the filling factor, a necessary quantity for testing equation (7). Generally speaking, the mass accretion rate is

$$\dot{M} = 4\pi R_*^2 f_{acc} \rho v, \quad (8)$$

where ρ is the density of the infalling material and v is the velocity at which it is coming in. Therefore,

$$f_{acc} = \frac{\dot{M}}{4\pi R_*^2 \rho v}. \quad (9)$$

HEG, GHBC, and WG01 all give \dot{M} and either R_* or the data necessary to derive it. One could either simply take single representative values for ρ and v or try to estimate them individually for each star. In either case though, the value of f_{acc} determined depends explicitly on the mass accretion rate. Therefore, one would naturally expect a good correlation between the left and right side of equation (7) since \dot{M} appears on both sides. We have estimated f_{acc} from equation (9) and do indeed find good correlations for equation (7), but this cannot be viewed as support for our extended version of the Ostriker and Shu (1995) model, so we do not include these plots for the data of HEG, GHBC, or WG01.

In summary then, we use data from 5 observational studies to look for the correlations predicted in equations (1), (2), and (7). Of these, 3 studies do not independently determine the filling factor of accretion spots, f_{acc} , and therefore are only suitable to test the relationships of the simple (dipole) accretion theories embodied in equation (1) and (2). These three studies are HEG, GHBC, and WG01. The investigations of VBJ and CG98 do independently estimate f_{acc} and are therefore suitable for testing the prediction of our modified Ostriker and Shu (1995) model, as well as the predictions of the simple models. Thus, VBJ and CG98 can be used to test equations (1), (2), and (7).

4. Analysis

4.1. Simple Accretion Theories

Figures 1a, 2, 3, 4a, and 5 show the results for the data from the 5 studies when looking for the correlation predicted by equation (1), which results from assuming a dipole magnetic field geometry with a constant field strength from star to star following Königl (1991), Shu et al. (1994 – and the unmodified Ostriker and Shu 1995 theory). In each figure, the quantity on the right hand side of the equation (1) is plotted versus the quantity on the left hand side of the equation. For simplicity in the plot units, we have expressed the stellar mass and radius in solar units for each star, and the mass accretion rate in units of $10^{-7} M_\odot \text{ yr}^{-1}$. As mentioned above, the scatter plots which result from equation (2) following Cameron and Campbell (1993) look almost identical to those shown in these figures and are therefore not shown separately. Filled circle

plot symbols denote single CTTs, and asterisks denote CTTs in binary systems. In all the figures, the expected correlation is shown with a dashed line. For those plots which do show a significant correlation (see below), the best fit line is shown in a solid line. In general, the expected relationship for equation (1) is only weakly present, with the data of HEG showing the strongest correlation.

We quantify these results by computing the linear correlation coefficient (also known as Pearson’s r) and its associated false alarm probability, P_f (Press et al. 1986). For each investigation, the associated correlation coefficient and false alarm probability are computed by using the logarithm of the quantities on each axis of the plots, thus giving the linear correlation of the scatter plots actually shown in these log-log plots. This is done to prevent the calculation of the correlation from being overly influenced by one or a few points with very large values on either axes. The resulting correlation coefficients and false alarm probabilities are given in Table 6. It is readily apparent from this table that when testing the correlations predicted by equations (1) or (2), only the HEG data produces a false alarm probability ≤ 0.01 , which is typically indicative of a real correlation. The data of HEG give $P_f = 0.009$ in the case of equation (2), suggestive of a significant correlation. The best fit line (solid line in the plot) is determined from a standard least squares analysis, assuming each data point has the same uncertainty in the y-axis quantity. To estimate the uncertainty in the slope (predicted to be 1 by the theory), we then use the best fit line to estimate observed residuals for each point. The standard deviation of these residuals is then assumed to be the 1σ uncertainty of each point in the y-axis quantity, which in turn gives an uncertainty for the slope in the least squares fit. Given the number of potential uncertainties that go into estimating the error bars for the points in each figure, we feel this means of estimating the final uncertainty of the slope from the scatter plots is the least biased. The slope and its uncertainty are given in Table 6 for that equation [(1), (2), or (7) discussed below] which produces the best correlation for each data set. For the case of HEG data and equation (2), the slope is 0.88 ± 0.29 which is insignificantly different from the expected value of 1.0.

4.2. Modified Ostriker and Shu

4.2.1. Initial Tests

Figures 1b and 4b show the results for the data from VBJ and CG98 respectively when looking for the correlation predicted by equation (7), which results from using the trapped flux concept of Ostriker and Shu (1995) while abandoning a pure dipole magnetic field geometry and assuming a constant stellar magnetic field strength. The plot symbols have the same meaning as given above, as do the solid and dashed lines. Both of these plots show much stronger correlations than present in the data when testing equations (1) and (2). This is also apparent in the correlation coefficients and false alarm probabilities given Table 6. Also given in the table is the best fit slope and uncertainty calculated in the same way as described above. The expected slope is 1.0 and the VBJ data give this slope to within the uncertainties. The CG98 data give a slope substantially below this expected value. This low slope is largely driven by the two stars with the lowest values of $R_*^2 f_{acc}$; however, excluding them still gives a slope which is too low at the 4σ level. This gives some concern, but as mentioned before (and discussed further below), CG98 do not actually fit their models to the observations, indicating that their study may not be the best suited for strictly testing the predicted correlations. Nevertheless, it is certainly true that equation (7) produces far better correlations in the data than either equations (1) or (2).

4.2.2. A Closer Look at VBJ and CG98

The data from both VBJ and CG98 appears to support the Ostriker and Shu (1995) theory as extended here to include non-dipole field topologies, while the data from all 5 observational studies at best only weakly supports the other magnetospheric accretion theories. As a result, it is important to look closely at VBJ and CG98 to see just how well they agree with equation (7). We also note from equation (8) that generally, \dot{M} depends on $f_{acc}R_*^2$, so there should be some correlation between these quantities. The observations primarily determine the accretion luminosity, L_{acc} , which is then used to determine the mass accretion rate either directly by applying an equation of the form

$$\dot{M} = \beta R_* L_{acc} / GM_* \quad (10)$$

where β depends on whether accretion occurs through an equatorial boundary layer or through a magnetosphere; or a model is used in the case of CG98 to fit the accretion luminosity and the resulting parameters give the mass accretion rate. At the same time, the filling factor, f_{acc} , is usually determined from the equation

$$L_{acc} = F_{acc} 4\pi R_*^2 f_{acc} \quad (11)$$

where F_{acc} is the emission per unit area from the accretion zones and is determined by fitting the observations to a model, either a hydrogen slab model in the case of VBJ or a shock model for CG98. Thus, both the determination of \dot{M} and f_{acc} primarily depend on L_{acc} and the value of R_* . Therefore, it is important to see how well \dot{M} is correlated with R_* (or R_*^2 , but when looking at the log of the quantities, it does not matter which power is considered when evaluating the correlation between \dot{M} and R_*) and f_{acc} separately, as well as with the product $R_*^2 f_{acc}$ to see if the correlations seen in Figures 1b and 4b are driven by these potential correlations. Indeed, CG98 point out that f_{acc} appears to be well correlated with \dot{M} in their study, making this a real concern. On the other hand, we already know that \dot{M} is not too well correlated with R_* since the top two panels in each figure do not show strong correlations.

In table 7 we give the correlation coefficients and resulting false alarm probabilities when comparing $\log(\dot{M}^{1/2})$ to $\log(f_{acc})$, $\log(R_*^2)$ and $\log(f_{acc}R_*^2)$ using the data from VBJ and CG98. These correlations are to be compared with the values in the last two columns of Table 6 which gives the correlation coefficient and false alarm probability when comparing all the parameters relevant to our extended Ostriker and Shu theory [$\log(M_*^{1/2} \dot{M}^{1/2} P_{rot}^{1/2})$ versus $\log(f_{acc}R_*^2)$]. In the case of VBJ, there is no correlation between the mass accretion rate and the filling factor, some between \dot{M} and R_*^2 and a real correlation between \dot{M} and $f_{acc}R_*^2$, but the full Ostriker and Shu (1995) comparison (Table 6) produces the best correlation. Thus, it appears that the inclusion of the rotation period and the mass do improve the results as predicted by the theory. The case is not quite the same for CG98, with the \dot{M} showing the best correlation with $f_{acc}R_*^2$, but the correlation based on equation (7) is nearly as high. It is certainly true that the CG98 shock model is the most physical of the two studies; however, CG98 do not actually fit the observed data, but pick by the eye the closest model from their grid to match the observations. It is also apparent from their Figure 6 that they do not generally match the observations (particularly the slope of the Paschen continuum) as well as VBJ, so it cannot be assumed that their values for various accretion parameters are more accurate.

We can look further at the results of VBJ. We substitute equation (10) into equation (7) to eliminate \dot{M} and then use equation (11) to eliminate f_{acc} . Dropping constants and re-arranging, we then find

$$R_*^{-1/2} L_{acc}^{1/2} \propto F_{acc} P_{rot}^{1/2}. \quad (12)$$

In the case of VBJ, F_{acc} is determined by a model fit and its value is largely driven by the shape of the Paschen continuum and the size of the Balmer jump. Equation (12) above involves parameters which are

independently determined to the greatest extent possible within the context of the VBJ study. The accretion luminosity is given by VBJ and we reproduce these in Table 1 for each star. Since we have access to the models used by VBJ, we compute F_{acc} by integrating over wavelength the excess flux produced by the best fitting hydrogen slab model for each star and also give these values in Table 1. We note that VBJ do not estimate f_{acc} using equation (11). Use of this equation with values of F_{acc} from Table 1 to estimate f_{acc} produce values which are systematically larger than those given by VBJ. The model of VBJ used the observations to determine the filling factor of the visible hemisphere (πR_*^2) covered by the boundary layer (accretion zones). The systematic difference between the two estimates of f_{acc} reflect the unknown foreshortening of the emitting region if it is not located at disk center on the stellar surface. This depends on the exact topology of the accretion and the limb darkening that should be applied. The two estimates of f_{acc} are extremely well correlated with each other and using values estimated from equation (11) produces a correlation in Figure 1b very similar to that shown. However, there are still worries that f_{acc} and \dot{M} may show an artificial correlation, so testing the relationship given in equation (12) is a better test of our modified version of the Ostriker and Shu (1995) theory. Figure 6 shows the two sides of equation (12) plotted against one another, showing an excellent correlation. The resulting correlation coefficient is $r = 0.92$ with an associated false alarm probability of $P_f = 1.5 \times 10^{-7}$. A least squares analysis finds a best fit line (shown in solid) in the log-log plot with a slope of 1.17 ± 0.12 which is not significantly different from the predicted slope of 1.0 (shown in the dashed line). We are unable to repeat this analysis for CG98 since we do not have access to their models. We can do a similar exercise for the data showing the highest correlation for the other magnetospheric accretion theories. Examining Table 6, the data from HEG may show a possible correlation when used to test equation (2). On the other hand, the HEG data shows a correlation between \dot{M} and R_* with $r = 0.75$ and $P_f = 3.1 \times 10^{-4}$. Again, using equation (10) to eliminate \dot{M} from equation (2) gives (after dropping constants)

$$R_*^{97/40} \propto M_*^{11/120} L_{acc}^{23/40} P_{rot}^{29/24}. \quad (13)$$

HEG tabulate L_{acc} for each star which we also give in Table 2. Using the HEG data to test equation (13) shows only a very weak correlation, with $r = 0.51$ and $P_f = 0.031$. The data are shown in Figure 7 and the slope is 0.88 ± 0.36 .

In summary, it appears both VBJ and CG98 are consistent with our extended version of the Ostriker and Shu (1995) theory, but the correlation given by CG98 may be the result of the generally expected correlation between \dot{M} and $f_{acc} R_*^2$. The data from VBJ actually show the best correlation when considering all the parameters required by the theory, and the data from this study shows an excellent correlation with the theory when one tries to remove the dependence of various parameters on each other. There is only weak support for the more general magnetospheric accretion theories of Königl (1991), Cameron and Campbell (1993), Shu et al. (1994), and Ostriker and Shu (1995) without the extensions described above for considering non-dipole field geometries.

4.2.3. Filling Factor Versus Stellar Radius

The above results suggest the Ostriker and Shu (1995) formulation can be shown to be consistent with the data if the strict dipole field geometry is dropped and it is assumed that the stellar magnetic field is basically constant from one CTTS to another. Ostriker and Shu (1995) state that one prediction of their work is that smaller CTTSs should have smaller filling factors of accretion spots on their surface. Thus we might expect f_{acc} and R_* to be directly related to one another. On the other hand, the relationship given in equation (7) above clearly predicts that f_{acc} and R_* should be inversely related to one another. This

apparent contradiction deserves some comment.

This result can be understood in terms of our equation (6), which was derived assuming a dipole field geometry in the vicinity of the truncation point of the disk, but which maps back to an arbitrarily complex field topology at the stellar surface. This equation certainly holds for a pure dipole as used by Ostriker and Shu (1995). Remembering that $A_* = 4\pi R_*^2 f_{acc}$, we can re-write equation (6) as

$$B_* R_*^2 f_{acc} = C_1 M_*^{1/2} \dot{M}^{1/2} P_{rot}^{1/2} \quad (14)$$

where C_1 is a constant, $C_1 = 2^{-5/2} \pi^{-1/2} G^{1/2} \Phi_{dx}$. If we now assume the field is a pure dipole as Ostriker and Shu (1995) do in their default model, then

$$B_* = \mu_* / R_*^{3+\epsilon} \quad (15)$$

where μ_* is the dipole moment of the star and ϵ is a small positive number ($0 < \epsilon < 1$) which takes into account the fact that as the stellar radius decreases, the relevant field lines which thread the disk truncation region in the Ostriker and Shu (1995) model are closer to the pole where the field strength is stronger. Putting this into equation (14) above yields:

$$\mu_* f_{acc} = R_*^{1+\epsilon} C_1 M_*^{1/2} \dot{M}^{1/2} P_{rot}^{1/2} \quad (16)$$

after some re-arrangement. Holding other things constant, you expect a direct relationship between f_{acc} and R_* as stated by Ostriker and Shu (1995). However, in our extension of the Ostriker and Shu (1995) theory to non-dipole field geometries at the stellar surface, equation (7) above clearly predicts an inverse relationship between f_{acc} and R_* if the magnetic field strength at the stellar surface is held constant along with the stellar mass, rotation period, and the mass accretion rate. In a log-log plot of f_{acc} versus R_* , equation (7) predicts a linear relationship with a slope of -2.

Figure 8 shows the relationship between the accretion filling factor, f_{acc} , and the stellar radius, R_* , for three data samples. The top panel uses the data given in Table 4 from CG98. This panel shows no correlation between the two quantities. This may simply reflect the fact that the other relevant parameters (M_* , \dot{M} , P_{rot}) must also be considered simultaneously; however, as mentioned above, the CG98 analysis does not strictly fit the observations, and in some case does not match the continuum slopes well. The middle panel of Figure 8 shows the VBJ data from Table 1. In this case an inverse correlation is observed: the correlation coefficient is $r = -0.72$ with an associated false alarm probability of $P_f = 1.1 \times 10^{-3}$. In a least squares analysis where we again use the distribution around the best fit line to estimate the uncertainty, the best fit slope is -1.70 ± 0.41 , which is not significantly different from the predicted value of -2 . The best fit is shown in a solid line, and the best fit with an assumed slope of -2 is shown in the dashed line.

One can test this relation using significantly more data points by using the entire sample of VBJ. The required filling factors are taken from Table 5 of VBJ, and the stellar radii are calculated from the stellar luminosities given in Table 5 of VBJ and the spectral types given in Table 1 of VBJ. Again, to translate spectral type into effective temperature, we use the calibration given by Johnson (1966). This entire data set consists of 43 stars which are plotted in the bottom panel of Figure 8. This figure again shows an obvious correlation which is borne out statistically ($r = 0.69$; $P_f = 9.3 \times 10^{-7}$). The best fit line (solid) has a slope of -1.65 ± 0.28 , which again is not significantly different from the predicted value of -2 (shown in the dashed line). We also see that in the entire data sample there is a large amount of scatter, particularly at the radius corresponding to the stars in the CG98 sample. Some of the scatter is likely due to the inherent variability of CTTS and some may also be due to the fact Figure 8 ignores the effects of other stellar parameters on the

correlation. Figure 8 also illustrates the need for a large data sample when making comparisons of this sort. The fact that we do see the predicted correlation in the full data set of VBJ with a slope very close to the predicted value suggests that our extension of the Ostriker and Shu (1995) theory may be a realistic way to relate the magnetic field in the X-region to the stellar surface. On the other hand, we note that there is an observational bias that also predicts $f_{acc} \propto R_*^{-2}$, which is shown in equation (11). For a larger star, a smaller filling factor of accretion shock emission is required to give the same area of emitting material, and hence the same luminosity, independent of exactly how the accreting material falls to the stellar surface. While the observed correlation is completely consistent with the prediction of our extended Ostriker and Shu (1995) model, it also suffers from a potential observational bias. Figure 6, based on equation (12), remains the strictest test of our modification to the Ostriker and Shu (1995) model, and it shows the best correlation found in this study.

5. Discussion

5.1. Results of This Study

The model of magnetically controlled accretion onto a compact object is encountered in many astrophysical contexts. In the case of CTTSs, such magnetospheric accretion appears to explain many of the properties of these stars; however, the general relationships between stellar and accretion parameters predicted by the theory has not been demonstrated observationally. In this paper, we use compilations of rotation periods and studies of accretion onto CTTSs from 5 sources (VBJ, HEC, GHBC, CG98, WG01) to test the general predictions of 4 analytic magnetospheric accretion models (Königl 1991, Cameron & Campbell 1993, Shu et al. 1994, and Ostriker & Shu 1995). All the theoretical studies assume a dipole configuration for the stellar magnetic field; however, Ostriker and Shu’s (1995) detailed analysis of the Shu et al. (1994) theory does not demand it. This treatment identifies the essential quantity of the trapped magnetic flux in the X-region, and this same amount of magnetic flux must thread the stellar surface in the accretion zones, independent of the exact magnetic topology on the stellar surface.

While magnetic field measurements for CTTSs are not numerous, those that are available show a surprising uniformity of the mean stellar field strength from star to star (Guenther et al. 1999, Johns–Krull et al. 1999b, Johns–Krull et al. 2001). Therefore, we have assumed a constant magnetic field from star to star and used data from the literature to look for the predicted correlations among stellar and accretion parameters which follow from the above mentioned theories. We suggest that a physical reason for the constancy of magnetic fields from one star to the other lies in a limit to the efficiency of the dynamo operating in these fully convective stars. Generally, the predicted correlations are absent or very weak in the data. This is also true of the strict Ostriker and Shu (1995) theory as applied to a pure dipole magnetic field geometry. On the other hand, Ostriker and Shu (1995) introduce the concept of the trapped flux, which allows one to abandon a strict dipole field geometry and still use the theory to make testable predictions (equations 6 and 7). In order to test these predictions, the filling factor, f_{acc} , of the accreting material on the stellar surface is required.

The studies of VBJ and CG98 are the only two considered here which present values for f_{acc} . For the stars in common in Tables 1 and 4, there is a large range in derived value of f_{acc} between the two studies for some stars. However, it is well known that CTTSs are quite variable, showing both rotational modulation of accretion signatures (e.g. Vrba et al. 1993, Johns & Basri 1995, Bouvier et al. 1999) as well as longer timescale variations in their accretion properties. In fact, Ardila and Basri (2000) find variations in the filling

factor on BP Tau with a full range from $f_{acc} = 0.00062 - 0.026$, a factor (42) comparable to the extremes found between VBJ and CG98. This suggests that the filling factor on CTTSs can vary substantially, which may account for much of the difference in the filling factors found by VBJ and CG98. On the other hand, for the stars in Tables 1 and 4, the filling factors derived by VBJ are larger by a median factor of 3.5 than those found by CG98, which may reflect a small systematic difference in the two studies. For their default model, Ostriker and Shu (1995) predict a filling factor $f_{acc} = 0.06$, comparable in value to many of the observed values. More reliable values of the filling factor would provide more stringent tests of the Ostriker and Shu (1995) model. Gómez de Castro and Lamzin (1999) show that analysis of ultraviolet (UV) emission lines in conjunction with shock models may result in tight constraints on accretion parameters. These results are promising, since the UV emission lines arise from the shock itself, as opposed to the photons being reprocessed through the photosphere as in the case of the optical excess studied by all five groups whose results are used in this paper. Unfortunately, the UV analysis has not yet proceeded to the point required to test the current magnetospheric accretion theories. The data in hand (Figures 1b and 4b) show much stronger correlations relative to the pure dipole accretion theories, with the VBJ data fully consistent with the predictions of equation (7). Uncertainties and variations in f_{acc} (as well as the other relevant parameters including P_{rot}) likely contribute to much of the observed scatter in the plots.

A closer look at the VBJ and CG98 data show that the VBJ data does support the Ostriker and Shu (1995) model when as many of the interdependencies of the various parameters as possible are removed. The CG98 data suggests that its apparent support for the extended Ostriker and Shu (1995) model may be the result of the expected correlation between the mass accretion rate and the area of the star participating in the accretion flow. On the other hand, none of the other magnetospheric accretion theories are well supported by the existing data, making the our extension of the Ostriker and Shu (1995) description the most viable of the current analytic theories. We note though that this study by no means rules out the work of Königl (1991), Cameron and Campbell (1993), or Shu et al. (1994) which employ strictly dipole field geometries. It may be that these models are essentially correct, and it is the dipole component of the field that varies from star to star in the manner required by the theory. We do note, however, that for the case of BP Tau (Johns–Krull et al. 1999a) and TW Hya (Johns–Krull & Valenti 2001) that the *measured* dipole components on these stars are substantially below the theoretically predicted values.

5.2. Implications

The apparent success of the Ostriker and Shu (1995) trapped flux model once a dipole geometry is abandoned, and the lack of success for the other theories which explicitly assume a dipole field geometry, suggests the magnetic fields on CTTSs are not large scale dipoles. Johns–Krull et al. (1999b) tabulate dipole field predictions for Königl (1991), Cameron and Campbell (1993), and Shu et al. (1994). Measured field *strengths* (Basri, Mary, & Valenti 1992; Guenther et al. 1999, Johns–Krull et al. 1999b, Johns–Krull et al. 2001) on TTSSs are in general agreement with these predictions; however, the dipole component of these fields appears to be smaller than the predictions by a factor of at least 10 in the case of Königl (1991) and Shu et al. (1994) based on the lack of detection of circular polarization in magnetically sensitive lines of CTTSs (Johns–Krull 1999a, Johns–Krull & Valenti 2001). The predicted dipole fields of Cameron and Campbell (1993) are weaker, but are still ruled out by the observations at the 6σ level, and the correlation analysis here does not generally support the Cameron and Campbell (1993) formulation. Independent of the theoretical predictions, the measured *strength* of the mean photospheric fields and the lack of observed circular polarization in the magnetically sensitive photospheric lines (Johns–Krull et al. 1999b, Johns–Krull

& Valenti 2001) indicates that the surface field topology on at least two CTTSs (BP Tau and TW Hya) is not dominated by a dipole. On the other hand, the dipole component of the stellar field will fall off the slowest with distance from the stellar surface and is likely to dominate at the disk truncation radius. We again note that this generally happens in the case of the solar magnetic field at $\sim 2.5R_{\odot}$ (Luhmann et al. 1998). This suggests that the material accreting onto the star generally does follow dipole-like magnetic field lines which explains the general success of line profile calculations done for dipole geometries (Hartmann, Hewett, & Calvet 1994; Muzerolle et al. 1998, 2001) as well as the circular polarization observed in the He I 5876 Å emission line of several CTTSs (Johns–Krull et al. 1999a, Johns–Krull & Valenti 2001).

It is interesting to briefly consider the study of Ferreira et al. (2000) which explores CTTS interactions with the surrounding disk for both dipole and higher order magnetic field components. This study is primarily concerned with the rotational spin down of young protostars into and through the TTS phase; however, the authors explicitly *ignore* the torque associated with the surrounding accretion disk. As a result, the results may not be accurate. In all their numerical results, Ferreira et al. (2000) find a (sometimes steep) increase in the stellar field strength as the star ages from 10^6 to 10^7 years and beyond. The limited magnetic field observations available do not currently support this picture: Johns–Krull and Valenti (2001) find a mean magnetic field on TW Hya (age 10^7 yr - Webb et al. 1999) which is well within the range found for CTTSs is Taurus. Additionally, Valenti and Johns–Krull (2001) report a mean field on a K3V Pleiades (age $\sim 10^8$ yr - Basri, Marcy, & Graham 1996) member which is *less* than those of TTS by about a factor of 2. More data is needed, particularly on young stars with an age of $\sim 10^7$ yr to see if any trends emerge.

We have just argued that the magnetic fields of CTTSs are not large scale dipoles and that the dipole component of CTTSs is significantly smaller than required by the magnetospheric accretion models of Königl (1991), Cameron & Campbell (1993), and Shu et al. (1994). Ostriker and Shu (1995) detail the theory of Shu et al. (1994) and show that the dipole assumption is not necessary by introducing the idea of trapped flux. How does the field strength in the trapped flux model compare with the observed field strength? Solving equation (6) for the stellar magnetic field gives:

$$B_* = 14,500 \left(\frac{M_*}{M_{\odot}} \right)^{1/2} \left(\frac{\dot{M}_D}{10^{-7} M_{\odot} \text{ yr}^{-1}} \right)^{1/2} \left(\frac{P_{rot}}{1 \text{ day}} \right)^{1/2} \left(\frac{R_*}{R_{\odot}} \right)^{-2} \left(\frac{f_{acc}}{0.01} \right)^{-1} \text{ G} \quad (17)$$

where we have set $A_* = 4\pi R_*^2 f_{acc}$. Since only the studies of VBJ and CG98 independently estimate the filling factor, f_{acc} , required in this equation, we only use these studies to estimate the stellar magnetic field strength, B_* . Table 8 gives these estimates for the 3 stars observed by Johns–Krull et al. (2001) for which the calculation can be made. Also given in the table is the observed mean field strength from Johns–Krull et al. (2001). It is important to note that in the analysis of Johns–Krull et al. (1999b, 2001) evidence is found for a range of field strengths on the surface of CTTSs, and we are unable to specify the field strength only in the accretion zone. The He I polarization data of Johns–Krull and Valenti (2000) and Valenti et al. (2001) probably probes the field in the accretion zone at the stellar surface, but there is an unknown inclination of this field to the line of sight which reduces the observed field strength below the actual field value. With these caveats, the predicted and observed field strengths agree to within a factor of 2-3, with the predictions using the parameters of VBJ generally falling below those based on the parameters of CG98 in this sample of 3 stars. Except for the rotation period, these two studies find different values for all the relevant parameters in equation (11); however, the one which is most significant in producing the difference in the predicted field strengths is the filling factor, f_{acc} . CTTSs are known to vary due to rotational modulation. In addition, there are also likely to be real changes in the instantaneous accretion rate onto the star (e.g. Ardila & Basri 2000). Both processes could change the apparent filling factor of accreting material. As a result (and as mentioned above), it is not clear that the difference in the derived filling factor values between VBJ and

CG98 is significant or simply the result of the variability of these stars.

Finally, we note that the relationships set forth in this paper are based on equilibrium calculations, while CTTs do show substantial variation. As a result, we expect that the relationships should hold for the mean value of the relevant parameters (particularly the accretion rate), but probably do not describe the relationship between these parameters as they vary over relatively short timescales (compared to the evolutionary timescale of CTTs and their disks). For example, Ardila and Basri (2000) study the accretion variability of the CTTs BP Tau, finding that $f_{acc} \propto \dot{M}^2$. At first, this appears to contradict equation (7). Rotational modulation may produce some of the variation observed by Ardila and Basri (2000). Aside from this, over the timescale of the variations in the instantaneous accretion rate studied by Ardila and Basri (2000), it is doubtful that the star reached a new equilibrium rotation rate which it would be expected to do. In other words, the torque balance on the star may also be varying, alternately trying to speed it up or slow it down, all the time varying around the equilibrium value. We would only expect equation (7) to hold for the mean values, as it seems to be based on the correlation plots presented in this paper. Indeed, some of the scatter seen in these plots is likely to result from the intrinsic variability displayed by CTTs.

6. Conclusions

The magnetospheric accretion model can explain many observed features of CTTs. Equilibrium models of this process have relied primarily on dipole field geometries to explore the interaction of the star with the disk, which seems appropriate since the dipole component should dominate at large distance from the star. Observations suggest that the magnetic fields of CTTs do not change much from star to star, though further observations are needed to confirm this. Under the assumption that the fields do not vary strongly, equilibrium theories predict specific correlations between stellar and accretion parameters which are generally not observed. This may mean that equilibrium theories are simply not adequate, or that a dipole field topology is too simple an assumption for relating observable parameters. On the other hand, we can use the notion of trapped flux introduced by Ostriker and Shu (1995) to extend this equilibrium theory to non-dipole field topologies at the stellar surface. The extension we make relies on assuming that the dipole component of the magnetic field does dominate at the X-region in the Ostriker and Shu (1995) model and that their analysis is accurate in terms of the accounting of how much magnetic flux is in the accretion flow, the dead zone, and the wind. This determines the magnetic flux in the accretion flow which we assume maps back to an equal amount of magnetic flux on the stellar surface. Again holding the magnetic field constant, new correlations are predicted between stellar and accretion parameters. We argue that the data of VBJ are the best suited for looking for these correlations, and that they are apparent in the data. This suggests that equilibrium models are adequate to describe the general features of magnetospheric accretion in CTTs once the dipole field assumption is dropped. Additional tests of our modified Ostriker and Shu (1995) model will confirm or refute this. Particularly valuable tests would be to determine all the relevant stellar and accretion parameters for stars with substantially different stellar properties than the Taurus stars used here. For example, detailed observations (including magnetic field measurements) of the more rapidly rotating CTTs in Orion could provide critical tests of equation (6) and (7). Tests of these equations will also benefit from better estimates of accretion rates and filling factors which may result from the analysis of UV emission lines produced in the accretion shock (e.g. Gómez de Castro & Lamzin 1999). Until then, it appears that our modified Ostriker and Shu (1995) is a reasonable description of magnetospheric accretion onto CTTs.

CMJ-K would like to acknowledge stimulating discussions with F. Shu and to thank him for pointing

out the role of the trapped flux. We acknowledge the careful reading of the manuscript by S. Mohanty and the useful discussions which resulted. Communications with L. Prato and R. White also provided important input on several issues raised in the manuscript. We also wish to thank an anonymous referee for feedback provided on this paper. CMJ-K and ADG both acknowledge partial support from a NASA Origins grant NAG5-8098 to the Regents of the University of California.

REFERENCES

- Alencar, S. H. P., Johns–Krull, C. M., & Basri, G., 2001, *AJ*, 122, 3335
- Ardila, D. R. & Basri, G. 2000, *ApJ*, 539, 834
- Armitage, P. J., Clarke, C. J., & Tout, C. A. 1999, *MNRAS*, 304, 425
- Artymowicz, P. & Lubow, S. H. 1994, *ApJ*, 421, 651
- Artymowicz, P. & Lubow, S. H. 1996, *ApJ*, 467, L77
- Basri, G., Marcy, G. W., & Graham, J. R. 1996, *ApJ*, 458, 600
- Basri, G., Marcy, G. W., & Valenti, J. A. 1992, *ApJ*, 390, 622
- Bertout, C., Basri, G., & Bouvier, J. 1988, *ApJ*, 330, 350
- Bertout, C., Harder, S., Malbet, F., Mennessier, C., & Regev, O. 1996, *AJ*, 112, 2159
- Bertout, C. & Mennessier, C. 1996, *Stellar Surface Structure*, K.G. Strassmeier & J.L. Linsky (eds.), IAU Symp. 176, 329
- Bouvier, J. 1990, *AJ*, 99, 946
- Bouvier, J., et al. 1999, *A&A*, 349, 619
- Bouvier, J., Cabrit, S., Fenandez, M., Martin, E.L., & Matthews, J.M. 1993, *A&A*, 272, 176
- Bouvier, J., Covino, E., Kovo, O., Martín, E.L., Matthews, J.M., Terranegra, L., & Beck, S.C. 1995, *A&A*, 299, 89
- Calvet, N. & Gullbring, E. 1998, *ApJ*, 509, 802 (CG98)
- Camenzind, M. 1990, *Rev. Modern Astron.*, (Berlin: Springer-Verlag), 3, 234
- Cameron, A. C. & Campbell, C. G. 1993, *A&A*, 274, 309
- Duchene, G., Monin, J.-L., Bouvier, J., & Menard, F. 1999, *A&A*, 351, 954
- Edwards, S., Hartigan, P., Ghandour, L., & Andrulis, C. 1994, *AJ*, 108, 1056
- Feigelson, E. D. & Montmerle, T. 1999, *ARAA*, 37, 363
- Ferreira, J., Pelletier, G., & Appl, S. 2000, *MNRAS*, 312, 387
- Ghez, A. M., White, R. J., & Simon, M. 1997, *ApJ*, 490, 353
- Ghez, A. M., Neugebauer, G., & Matthews, K. 1993, *AJ*, 106, 2005
- Ghosh, P. 1995, *MNRAS*, 272, 763
- Ghosh, P. & Lamb, F. K. 1979, *ApJ*, 232, 259
- Gómez de Castro, A. I. & Lamzin, S. A. 1999, *MNRAS*, 304, L41
- Goodson, A. P., Böhm, K.-H., & Winglee, R. M. 1999, *ApJ*, 524, 142
- Goodson, A. P., Winglee, R. M., & Böhm, K.-H. 1997, *ApJ*, 489, 199
- Guenther, E. W., Lehmann, H., Emerson, J. P., & Staude, J. 1999, *A&A*, 341, 768
- Gullbring, E., Hartmann, L., Briceño, C., & Calvet, N. 1998, *ApJ*, 492, 323 (GHBC)
- Hartigan, P., Edwards, S., & Ghandour, L. 1995, *ApJ*, 452, 736 (HEG)
- Hartmann, L., Hewett, R., & Calvet, N. 1994, *ApJ*, 426, 669
- Hartmann, L. & Stauffer, J. R. 1989, *AJ*, 97, 873

- Herbst, W., Bailer–Jones, C. A. L., & Mundt, R. 2001, *ApJ*, 554, L197
- Hayashi, M. R., Shibata, K., & Matsumoto, R. 1996, *ApJ*, 468, L37
- Johns, C. M. & Basri, G. 1995, *ApJ*, 449, 341
- Johns–Krull, C. M. & Valenti, J. A. 2000, *Stellar Clusters and Associations: Convection, Rotation, and Dynamos*, (eds.) R. Pallavicini, G. Micela, & S. Sciuto, *ASP Conf. Series*, 198, p. 371
- Johns–Krull, C. M. & Valenti, J. A. 2001, *Young Stars Near Earth: Progress and Prospects*, (eds.) R. Jayawardhana & T. Greene, *ASP Conference Series*, 244, 147
- Johns–Krull, C. M., Valenti, J. A., Hatzes, A. P., & Kanaan, A. 1999a, 510, L41
- Johns–Krull, C. M., Valenti, J. A., & Koresko, C. 1999b, *ApJ*, 516, 900
- Johns–Krull, C. M., Valenti, J. A., Saar, S. H., & Hatzes, A. P. 2001, *Cool Stars, Stellar Systems, and the Sun: 11th Cambridge Workshop*, R. J. García López, R. Rebolo, & M. R. Zapatero Osorio (eds.), *ASP Conf. Series*, 223, 521
- Johnson, H. L. 1966, *ARAA*, 4, 193
- Koide, S., Shibata, K., & Kudoh, T. 1999, *ApJ*, 522, 727
- Königl, A. 1991, *ApJ*, 370, L39
- Königl, A. & Pudritz, R. E. 2000, *Protostars & Planets IV*, (eds.) V. Mannings, A. P. Boss, & S. S. Russell, (Arizona: Tucson), p. 759
- Kenyon, S. J., Hartmann, L., Hewett, R., Carrasco, L., Cruz–Gonzalez, I., Recillas, E., Salas, L., Serrano, A., Strom, K. M., Strom, S. E., & Newton, G. 1994, *AJ*, 107, 2153
- Lamzin, S. A. 1995, *A&A*, 295, L20
- Luhmann, J. G., Gosling, J. T., Hoeksema, J. T., & Zhao, X. 1998, *J. Geophys. Res.*, 103, 6585
- Mathieu, R. D. 1994, *ARAA*, 32, 465
- Miller, K. A. & Stone, J. M. 1997, *ApJ*, 489, 890
- Muzerolle, J., Calvet, N., Briceño, C., Hartmann, L., & Hillenbrand, L. 2000, *ApJ*, 535, L47
- Muzerolle, J., Calvet, N., & Hartmann, L. 1998, *ApJ*, 492, 743
- Muzerolle, J., Calvet, N., & Hartmann, L. 2001, *ApJ*, 550, 944
- Ostriker, E. C. & Shu, F. H. 1995, *ApJ*, 447, 813
- Ostriker, E. C., Shu, F. H., & Adams, F. C. 1992, *ApJ*, 399, 192
- Paatz, G. & Camenzind, M. 1996, *A&A*, 308, 77
- Press, W. H., Flannery, B. P., Teukolsky, S. A., & Vetterling, W. T. 1988, *Numerical Recipes*, (New York: Cambridge Univ. Press), 277
- Shu, F. H., Najita, J., Ostriker, E., Wilkin, F., Ruden, S., & Lizano, S. 1994, *ApJ*, 429, 781
- Simon, M. & Prato, L. 1995, *ApJ*, 450, 824
- Stassun, K. G., Mathieu, R. D., Mazeh, T., & Vrba, F. J. 1999, *AJ*, 117, 2941
- Valenti, J. A., Basri, G., & Johns, C. M. 1993, *AJ*, 106, 2024 (VBJ)
- Valenti, J. A. & Johns–Krull, C. 2001, *Magnetic Fields Across the Hertzsprung–Russell Diagram*, (eds.) G. Mathys, S. K. Solanki, & D. T. Wickramasinghe, *ASP Conf. Series*, 248, 179

- Valenti, J. A., Johns–Krull, C. M., & Hatzes, A. P. 2001, *ApJ*, in preparation
- Vrba, F. J., Chugainov, P. F., Weaver, B. W., & Stauffer, J. S. 1993, *AJ*, 106, 1608
- Webb, R. A., Zuckerman, B., Platais, I., Patience, J., White, R. J., Schwartz, M. J., & McCarthy, C. 1999, *ApJ*, 512, L63
- White, R. J. & Ghez, A. M. 2001, *ApJ*, 556, 265 (WG01)
- White, N. E. & Stella, L. 1988, *MNRAS*, 231, 325
- Wickramasinghe, D. T. & Ferrario, L. 2000, *New Astron. Rev.*, 44, 69

Fig. 1.— (a) The top panel shows the quantity $(M_*/M_\odot)^{5/6}(\dot{M}/1 \times 10^{-7}M_\odot yr^{-1})^{1/2}P_{rot}^{7/6}$ versus $(R_*/R_\odot)^3$ for the sample of stars from VBJ. Single CTTSs are shown in solid circles while CTTSs in binary systems are shown in asterisks. The dashed line shows the best fit line whose slope (1.0) is predicted by equation (1). (b) The bottom panel shows the quantity $(M_*/M_\odot)^{1/2}(\dot{M}/1 \times 10^{-7}M_\odot yr^{-1})^{1/2}P_{rot}^{1/2}$ versus $(R_*/R_\odot)^2 f_{acc}$ for the sample of stars from VBJ. Plot symbols are the same as in panel (a). Shown in the solid line is the best fit line to the data, and shown in the dashed line is best fit line whose slope (1.0) is predicted by equation (7).

Fig. 2.— Same as Figure 1a but using the data of HEG. Also shown in the solid curve is the best fit line to the data.

Fig. 3.— Same as Figure 1a but using the data of GHBC.

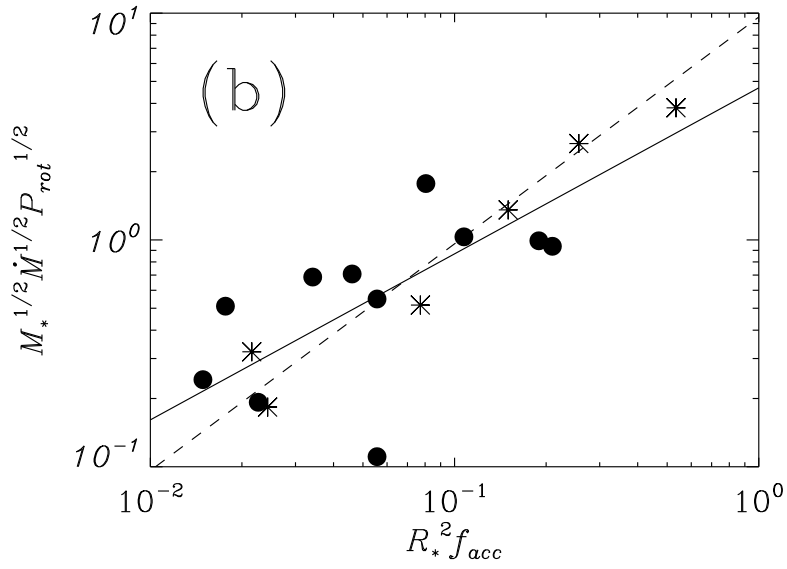
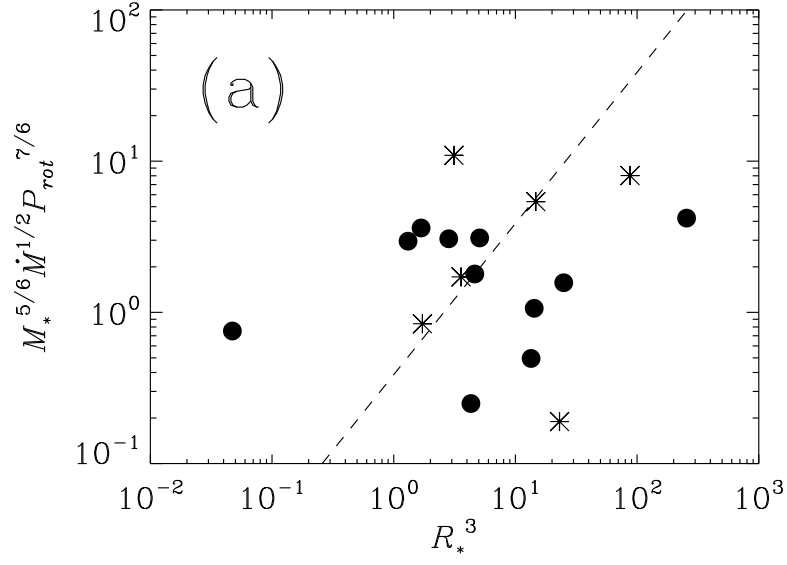
Fig. 4.— Same as Figure 1 but using the data of CG98.

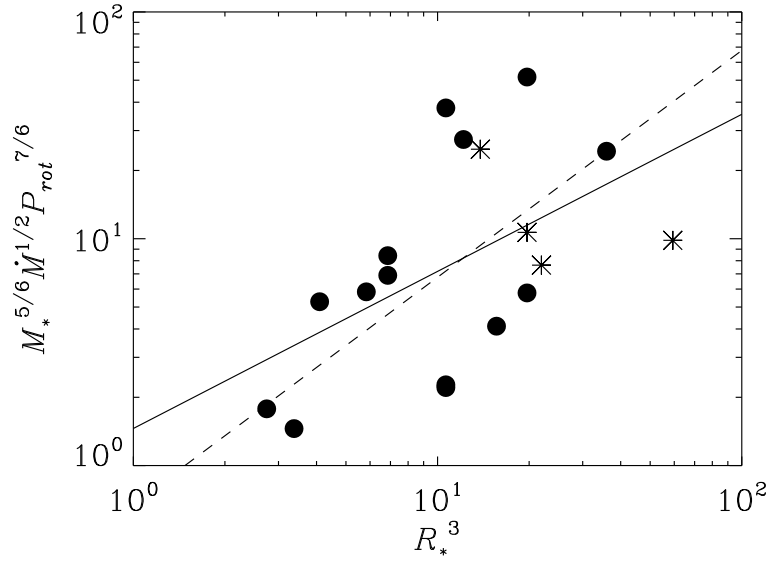
Fig. 5.— Same as Figure 1a but using the data of WG01.

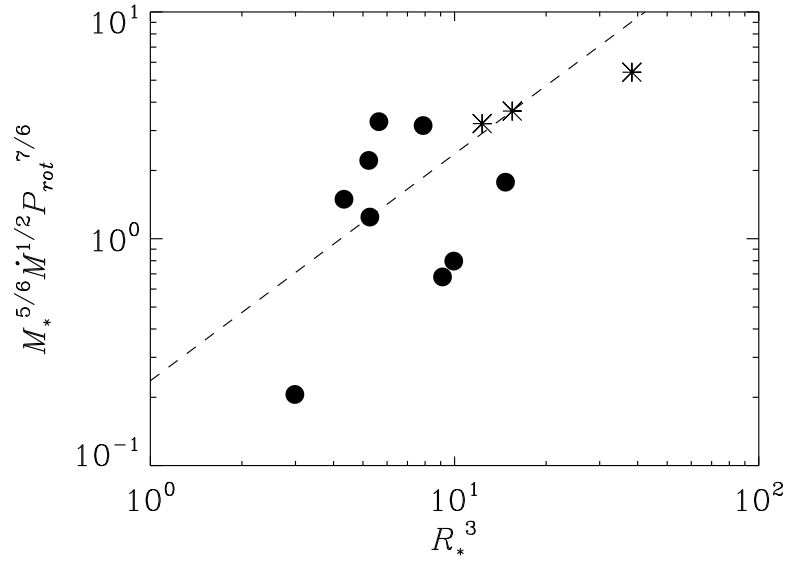
Fig. 6.— The data from VBJ are used to test for the correlation predicted by equation (12). The dashed line shows the best fit match to the points keeping the slope fixed to the value predicted in equation (12), while the best fit line with a free slope is shown in the solid line.

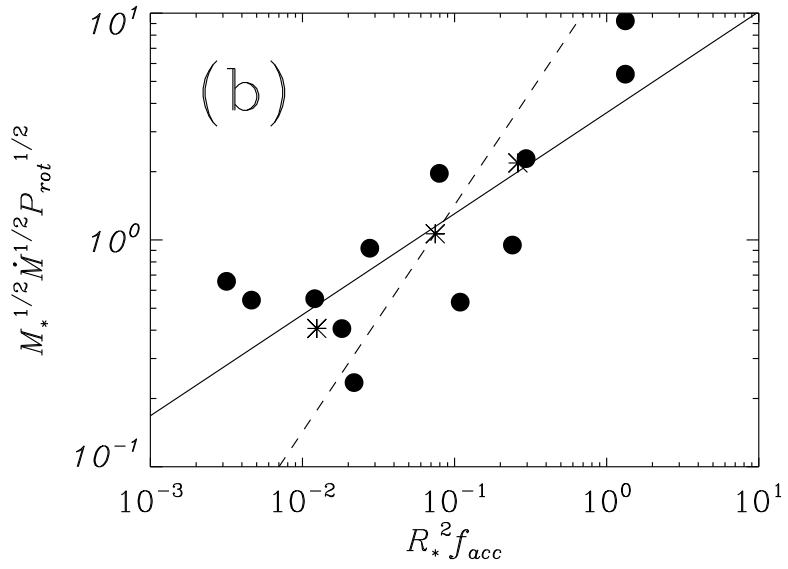
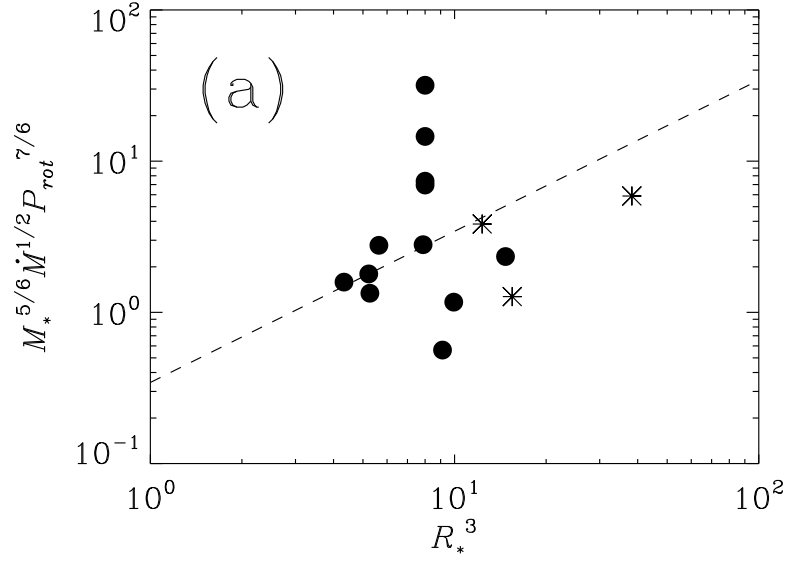
Fig. 7.— The data from HEG are used to test for the correlation predicted by equation (13). The dashed line shows the best fit match to the points keeping the slope fixed to the value predicted in equation (13), while the best fit line with a free slope is shown in the solid line.

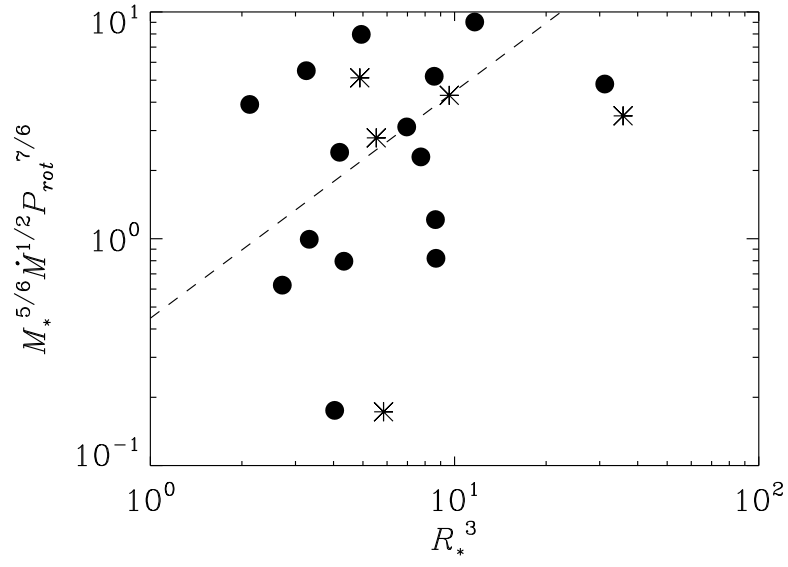
Fig. 8.— The accretion filling factor, f_{acc} , versus the stellar radius, R_* , for three data samples. The upper panel uses the data of CG98 as given in this paper. The middle panel is data from VBJ as given in this paper, and the lower panel is the full set of VBJ data. Again, single CTTSs are shown as solid circles and those in binary systems are shown as asterisks. In each panel, the dashed line is the best fit line with an assumed slope of -2 (the predicted slope). In the lower two panels where real correlations do exist, the best fit line is plotted in the solid line. In these two panels, the best fit line is not significantly different from the expected relationship.

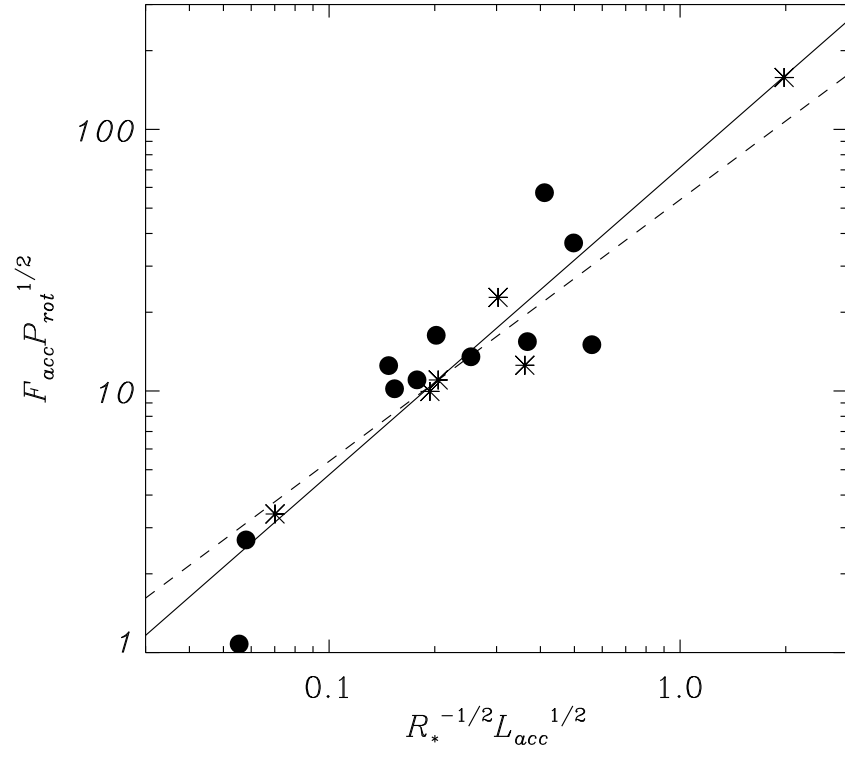


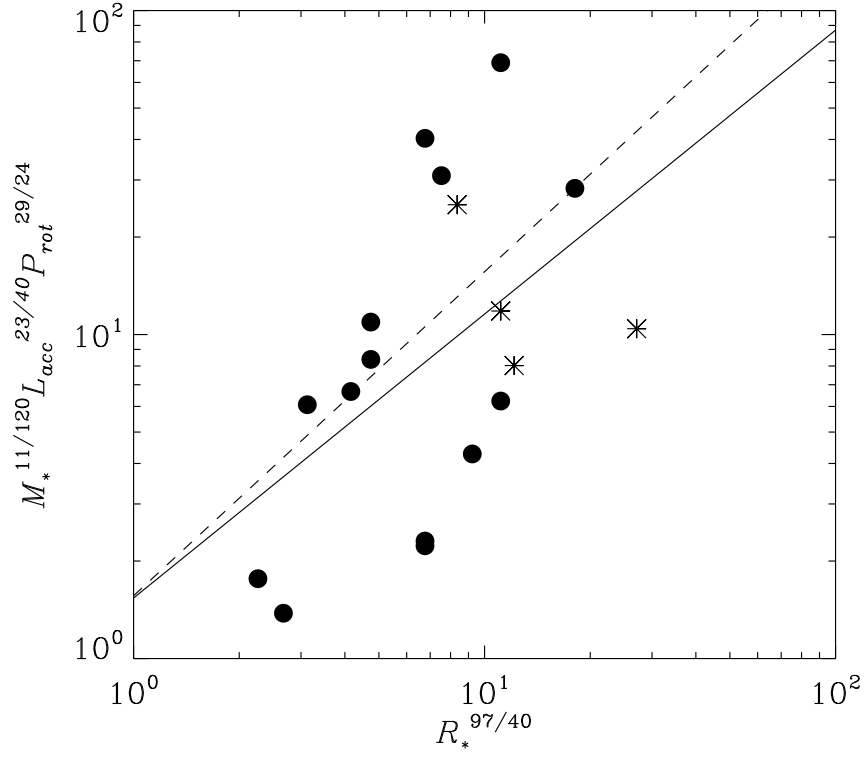












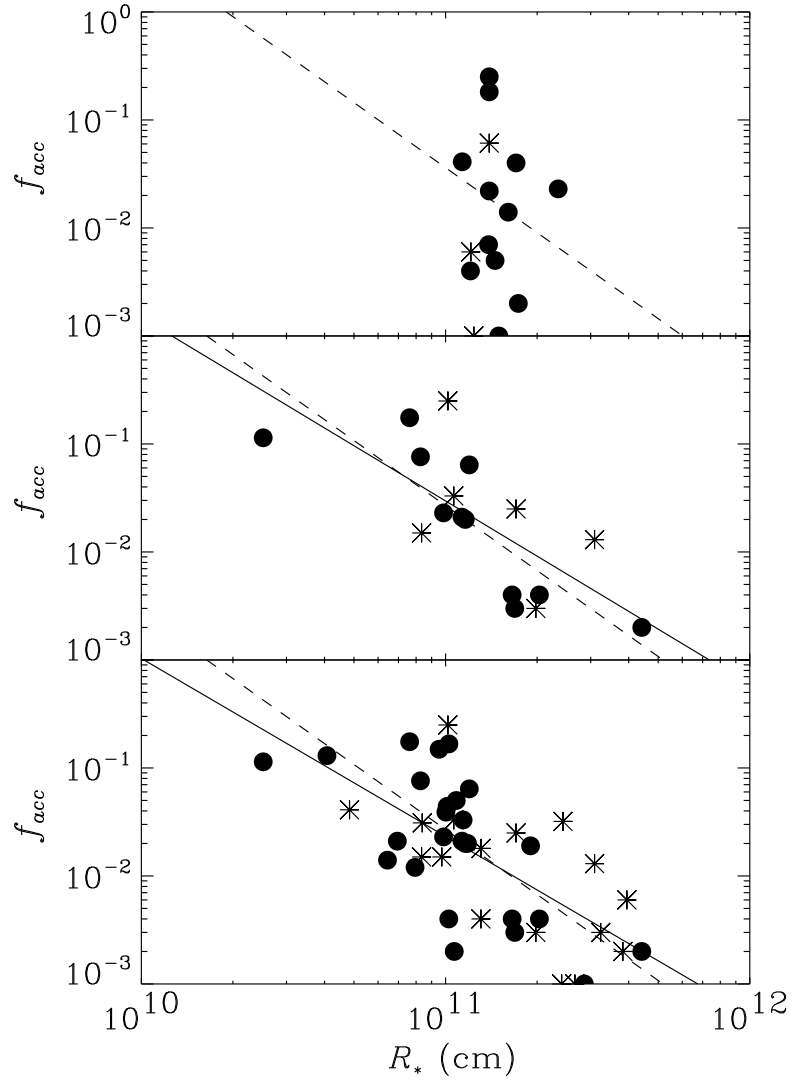


Table 1. VBJ Sample of Stars

Star	T_{eff} (K)	M_* (M_\odot)	R_*^a (R_\odot)	$\dot{M} \times 10^7$ ($M_\odot \text{yr}^{-1}$)	f_{acc}	P_{rot} (days)	$\frac{L_{acc}}{L_\odot}$	$F_{acc} \times 10^{-10}$ ($\text{erg cm}^{-2} \text{s}^{-1}$)
AA Tau	4000	0.52	1.67	0.071	0.020	8.20	0.068	5.7
BP Tau	4000	0.53	1.72	0.243	0.064	7.60	0.232	5.6
CW Tau	4775	0.45	0.36	0.016	0.114	8.20	0.061	20.
DE Tau	3400	0.23	6.34	1.796	0.002	7.60	0.201	4.0
DF Tau ^b	3675	0.38	4.43	2.192	0.013	8.50	0.579	4.3
DH Tau	3600	0.23	2.92	0.283	0.004	7.20	0.069	3.8
DK Tau ^b	4000	0.52	1.53	0.061	0.033	8.40	0.064	3.8
DL Tau	4000	0.49	1.19	0.233	0.076	9.40	0.294	12.
DN Tau	3750	0.47	2.39	0.013	0.004	6.00	0.008	1.1
GG Tau A ^b	4000	0.59	2.45	0.301	0.025	10.30	0.225	7.1
GI Tau	4200	0.60	1.09	0.202	0.175	7.20	0.344	5.6
GK Tau	4000	0.53	1.63	0.005	0.021	4.65	0.005	0.5
GM Aur	4775	0.56	1.42	0.074	0.023	12.00	0.091	3.9
HP Tau ^b	4775	0.51	1.20	0.034	0.015	5.90	0.045	4.1
IQ Tau	3675	0.23	2.43	0.180	0.003	6.25	0.053	5.0
RW Aur AB ^b	5100	0.80	1.46	3.384	0.250	5.39	5.725	68.
XZ Tau ^b	3300	0.16	2.85	0.079	0.003	2.60	0.014	2.1

^aCalculated from stellar luminosity and effective temperature.

^bDenotes a star in a binary system.

Table 2. HEG Sample of Stars

Star	T_{eff} (K)	M_* (M_\odot)	R_* (R_\odot)	$\dot{M} \times 10^7$ ($M_\odot \text{yr}^{-1}$)	P_{rot} (days)	$\log(\frac{L_{acc}}{L_\odot})$
AA Tau	3800	0.38	1.8	1.26	8.20	-0.42
BP Tau	4000	0.45	1.9	1.58	7.60	-0.19
CW Tau	4730	1.03	2.2	10.00	8.20	0.87
CY Tau	4000	0.58	1.4	0.06	7.90	-1.42
DE Tau	3570	0.24	2.7	3.16	7.60	-0.37
DF Tau ^a	3500	0.17	3.9	12.59	8.50	-0.06
DG Tau	4395	0.67	2.3	19.95	6.30	0.94
DK Tau ^a	4000	0.38	2.7	3.98	8.40	-0.01
DL Tau	3800	0.37	1.9	2.00	9.40	-0.17
DN Tau	4000	0.42	2.2	0.32	6.00	-0.97
DR Tau	4000	0.38	2.7	79.43	9.00	1.26
GG Tau A ^a	3800	0.29	2.8	2.00	10.30	-0.47
GI Tau	3800	0.30	2.5	1.26	7.20	-0.62
GK Tau	4000	0.41	2.2	0.63	4.65	-0.71
GM Aur	4000	0.52	1.6	0.25	12.00	-0.86
RW Aur ^a	4000	0.85	2.4	15.85	5.39	0.91
V836 Tau	4000	0.54	1.5	0.06	7.00	-1.49
YY Ori	4000	0.34	3.3	31.62	7.58	0.75

^aDenotes a star in a binary system.

Table 3. GHBC Sample of Stars

Star	T_{eff} (K)	M_* (M_\odot)	R_* (R_\odot)	$\dot{M} \times 10^7$ ($M_\odot \text{yr}^{-1}$)	P_{rot} (days)
AA Tau	3800	0.53	1.74	0.033	8.20
BP Tau	4000	0.49	1.99	0.288	7.60
CY Tau	4000	0.42	1.63	0.075	7.90
DE Tau	3570	0.26	2.45	0.264	7.60
DF Tau ^a	3500	0.27	3.37	1.769	8.50
DK Tau ^a	4000	0.43	2.49	0.379	8.40
DN Tau	4000	0.38	2.09	0.035	6.00
GG Tau A ^a	3800	0.44	2.31	0.175	10.30
GI Tau	3800	0.67	1.74	0.096	7.20
GK Tau	4000	0.46	2.15	0.064	4.65
GM Aur	4000	0.52	1.78	0.096	12.00
IP Tau	3750	0.52	1.44	0.008	3.25

^aDenotes a star in a binary system.

Table 4. CG98 Sample of Stars

Star	T_{eff}^a (K)	M_*^a (M_\odot)	R_*^a (R_\odot)	$\dot{M} \times 10^{7b}$ ($M_\odot \text{yr}^{-1}$)	f_{acc}	P_{rot} (days)
AA Tau	3800	0.53	1.74	0.04	0.006	8.20
BP Tau	4000	0.49	1.99	0.23	0.007	7.60
CW Tau	4730	0.50	2.00	1.27	0.061	8.20
CY Tau	4000	0.42	1.63	0.08	0.041	7.90
DE Tau	3570	0.26	2.45	0.46	0.040	7.60
DF Tau ^c	3500	0.27	3.37	2.08	0.023	8.50
DG Tau	4395	0.50	2.00	9.19	0.251	6.30
DK Tau ^c	4000	0.43	2.49	0.05	0.002	8.40
DL Tau	3800	0.50	2.00	0.82	0.022	9.40
DN Tau	4000	0.38	2.09	0.02	0.005	6.00
DR Tau	4000	0.50	2.00	19.01	0.182	9.00
GG Tau A ^c	3800	0.44	2.31	0.25	0.014	10.30
GI Tau	3800	0.67	1.74	0.06	0.004	7.20
GK Tau	4000	0.46	2.15	0.14	0.001	4.65
GM Aur	4000	0.52	1.78	0.07	0.001	12.00

^aTaken from GHBC except for CW Tau, DL Tau, DG Tau, and DR Tau which are assumed by CG98 to have $M_* = 0.5M_\odot$ and $R_* = 2.0R_\odot$.

^bCalculated from equation (11) of CG98.

^cDenotes a star in a binary system.

Table 5. WG01 Sample of Stars

Star	T_{eff} (K)	M_* (M_\odot)	R_* ^a (R_\odot)	$\dot{M} \times 10^7$ ($M_\odot \text{yr}^{-1}$)	P_{rot} (days)
AA Tau	4000	0.78	1.61	0.06	8.20
BP Tau	4000	0.77	1.91	0.13	7.60
CW Tau	4775	1.06	1.28	0.10	8.20
CY Tau	3400	0.55	1.63	0.01	7.90
DE Tau	3600	0.66	3.15	0.41	7.60
DF Tau A ^b	3775	0.68	1.77	0.10	8.50
DG Tau	4200	0.88	2.05	0.07	6.30
DH Tau	3400	0.53	1.39	0.01	7.20
DL Tau	4000	0.77	2.27	0.68	9.40
DN Tau	3750	0.70	2.06	0.02	6.00
DR Tau	4400	1.11	1.70	0.32	9.00
GG Tau Aa ^b	4000	0.76	2.13	0.13	10.3
GI Tau	4000	0.76	1.98	0.08	7.20
GK Tau	4000	0.76	2.05	0.06	4.65
GM Aur	4775	1.22	1.48	0.07	12.00
IP Tau	3750	0.71	1.59	0.003	3.25
LkCa 15	4400	1.05	1.49	0.01	5.85
RW Aur A ^b	5080	1.34	1.70	0.32	5.39
T Tau A ^b	5250	2.11	3.30	0.32	2.80
XZ Tau A ^b	3410	0.44	1.80	0.01	2.60

^aCalculated from stellar luminosity and effective temperature.

^bDenotes a star in a binary system.

Table 6. Correlation Coefficients and False Alarm Probabilities

Dataset	$r(1)$	$P_f(1)$	$r(2)$	$P_f(2)$	$r(7)$	$P_f(7)$	Slope
VBJ	0.17	0.508	0.24	0.350	0.79	1.5×10^{-4}	0.73 ± 0.14
HEG	0.52	0.026	0.59	9.4×10^{-3}	0.88 ± 0.29
GHBC	0.61	0.034	0.67	0.018	0.99 ± 0.34
CG98	0.11	0.690	0.16	0.570	0.82	1.7×10^{-4}	0.45 ± 0.10
WG01	0.28	0.225	0.30	0.198	0.45 ± 0.35

Note. — The correlation coefficient, r , and associated false alarm probability, P_f , are given for each studies testing of the relationships given in equations (1), (2), and (7).

Table 7. Correlating f_{acc} and R_* with \dot{M} Using VBJ and CG98

Comparison	$r(VBJ)$	$P_f(VBJ)$	$r(CG98)$	$P_f(CG98)$
$\dot{M}^{1/2}$ vs. f_{acc}	0.06	0.82	0.81	2.5×10^{-4}
$\dot{M}^{1/2}$ vs. R_*^2	0.50	0.041	0.28	0.319
$\dot{M}^{1/2}$ vs. $f_{acc}R_*^2$	0.69	2.3×10^{-3}	0.84	8.9×10^{-5}

Table 8. Observed and Predicted Magnetic Fields

Star	$B_*(obs)$ (kG)	$B_*(VBJ)$ (kG)	$B_*(CG98)$ (kG)
BP Tau	2.10	0.76	4.85
DF Tau	2.30	1.52	1.22
DK Tau	2.70	0.98	4.99